Virginia Commonwealth University
VCU Scholars Compass

Electrical and Computer Engineering Publications

Dept. of Electrical and Computer Engineering

2006

Effect of C/Si ratio on deep levels in epitaxial 4H–SiC

C. W. Litton
Air Force Research Laboratory, cole.litton@sbcglobal.net

D. Johnstone
SEMETROL

S. Akarca-Biyikli
Virginia Commonwealth University

See next page for additional authors

Follow this and additional works at: http://scholarscompass.vcu.edu/egre_pubs

Part of the Electrical and Computer Engineering Commons

Downloaded from

http://scholarscompass.vcu.edu/egre_pubs/117

Authors

C. W. Litton, D. Johnstone, S. Akarca-Biyikli, K. S. Ramaiah, I. Bhat, T. P. Chow, J. K. Kim, and E. F. Schubert

Effect of C/Si ratio on deep levels in epitaxial 4H–SiC

C. W. Litton[a)]
Air Force Research Laboratory, Materials and Manufacturing Directorate (AFRL/MLPS),
Wright–Patterson Air Force Base, Ohio 45433

D. Johnstone
SEMETROL, 13312 Shore Lake Turn, Chesterfield, Virginia 23838

S. Akarca-Biyikli
Department of Electrical Engineering, Virginia Commonwealth University, Richmond, Virginia 23284

K. S. Ramaiah, I. Bhat, T. P. Chow, J. K. Kim, and E. F. Schubert
Department of Electrical, Computer and System Engineering, Rensselaer Polytechnic Institute,
110 8th Street, Troy, New York 12180

Changing the ratio of carbon to silicon during the epitaxial 4H–SiC growth is expected to alter the dominant deep level trap, which has been attributed to a native defect. The C/Si ratio was changed from one to six during epitaxial growth of SiC. Diodes fabricated on the epitaxial layer were then characterized using current-voltage and deep level transient spectroscopy. The single peak at 340 K (Z1/Z2 peak), was deconvolved into two traps, closely spaced in energy. The concentration of one of the Z1/Z2 traps decreased with increasing C/Si ratio. This result opposes theoretical predictions of carbon interstitial components, and supports assignment to a silicon antisite or carbon vacancy relationship. The concentration of the second component of the peak at 340 K did not depend on the C/Si ratio, which would indicate an impurity in an interstitial site. © *2006 American Institute of Physics.* [DOI: 10.1063/1.2161388]

Both 4H and 6H polytypes of SiC have a defect at $0.6–0.7$ eV below the conduction band, and this is a dominant defect in 4H–SiC. Various models have been proposed for the composition of this Z1/Z2 defect, and various experimental studies have also been performed,[1] primarily based on generating intrinsic defects by irradiation.[2] In this work, we have characterized the Z1/Z2 defect in detail by fabricating Schottky diodes on a C-face 4H–SiC grown under different carbon to silicon ratios.

Epitaxial growth of SiC on C-face 4H–SiC substrates was carried out in a horizontal low-pressure coldwall reactor. The (000-1) 4H–SiC substrates, misoriented 8° toward $[11\bar{2}0]$ ($n \sim 10^{18}$ cm^{-3}), obtained from Cree Research, Inc., were cleaned sequentially in acetone, xylene, and methanol using an ultrasonic bath, then cleaned with Caro's etch (H_2SO_4:H_2O_2:H_2O), rinsed in deionized water, and finally dried in N_2. Prior to the epitaxial deposition, the substrates were etched in H_2/propane mixture at ~ 1400 °C for 10 min. Silane (2% SiH$_4$ in H$_2$), and propane (2% C$_3$H$_8$ in H$_2$) were used as the precursors for Si and C, respectively. Palladium purified H$_2$ was used as the carrier gas. Nitrogen (2% N$_2$ in H$_2$) was used as the *n*-type dopant. The substrate temperature and the reactor pressure were kept at 1550 °C and 80 Torr, respectively. The C/Si ratio was varied from 1.0 to 6.0 by changing the propane flow, keeping the silane flow constant.

Schottky junctions were fabricated on 5 μm thick epitaxial layers employing shadow mask with hole diameters of 0.5, 1.0, and 1.5 mm. To make ohmic contact to the back side, Ti(200 Å)/Ni(800 Å)/Al(100 Å) metals were deposited by electron-beam evaporation and then annealed at 1000 °C for 5 min in Ar by rapid thermal processing. Ni

(300 Å)/Au(500 Å) metals were deposited through the shadow mask on the front surface for Schottky contacts. The rectifying properties of the Schottky contacts were improved further by annealing the samples at 500 °C for 15–20 min in Ar.

The carrier concentration in the samples was measured by C–V as 6.6×10^{15}/cm^3 for the sample grown with C/Si of one, and 1.5×10^{15} cm^3 for the C/Si of three and six. Figure 1 shows the current-voltage (*I-V*) characteristics of Schottky diodes fabricated on layers grown with different C/Si ratio. The reverse bias current is the lowest for the C/Si ratio of three. A plot of the current versus (voltage)$^{0.5}$
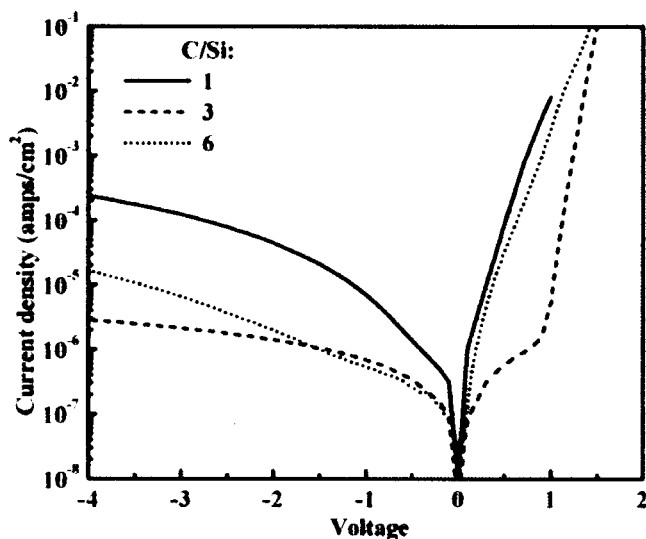

FIG. 1. The *I-V* characteristics of Schottky diodes fabricated on layers grown with different C/Si ratios.

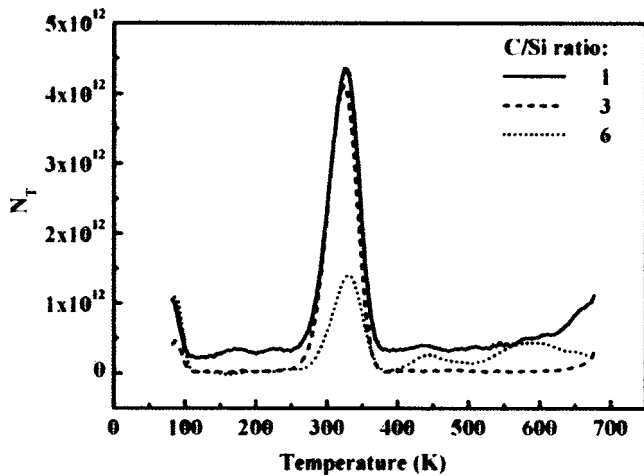a)Electronic mail: cole.litton@sbcglobal.net

FIG. 2. DLTS spectra from *n*-type 4H–SiC grown with different carbon to silicon ratios of one, three, and six. The ratewindow time constant is 228 s.

(not shown), proportional to the volume of generation centers, was superlinear for each of the samples, pointing out that the dominant mechanism is not via a generation center, in which case the reverse bias current would be expected to scale linearly with the volume of the depletion region.

From the deep-level transient spectroscopy (DLTS) measurements, a ratewindow plot of the spectra from each of the samples, grown with carbon to silicon ratios of one, three, and six, is shown in Fig. 2. The spectra all show the same features, although in different proportions, dominated by the Z1/Z2 trap at 330 K. Increasing the C/Si ratio from one to three did not result in an appreciable change in the trap concentration, where the trap concentration is given by the peak height. However, increasing the ratio to six resulted in a decrease in the Z1/Z2 trap concentration by a factor of 3. Note that the spectrum for the C/Si ratio of one has higher series resistance than the other two, and required a correction factor, increasing the spectrum by 30%, according to[3]

$$\Delta C_m = \frac{\Delta C}{[1 + (r_s C\omega)^2]} \left\{ 1 - \frac{2(r_s C\omega)^2}{[1 + (r_s C\omega)^2]} \right\}.$$

The other two samples had series resistances in the range of 10 Ω, which has a negligible effect on the measured capacitance. The Arrhenius plot shown in Fig. 3 is obtained by plotting the emission rate factor, adjusted by T^2 for the temperature dependence of the thermal velocity and the conduction band density of states, versus $1/kT$.[4,5] The emission rate is extracted from a fit of the capacitance transient. The energies and capture cross sections, and trap concentrations are given in Table I. The designations used are the same as in Ref. 6. The energy and capture cross section are taken from the slope and intercept of the Arrhenius plot. The concentration is taken from the amplitude of the transients, corrected for the volume scanned. The volume was determined from the depletion width at the biases used for filling and measurement, from the capacitance-voltage profile, and the diameter of the diode. In each case, 0.0 V was used for the filling pulse, and −2.0 V was used for the measurement bias. The filling pulse width was 10 ms for each.

The trap at 0.17 eV has been reported as due to Ti in a cubic site.[6,7] The capacitance transients used to generate the single Z1/Z2 peak at 320 K in the ratewindow plot, were best fit for two exponential components, given in Table I as
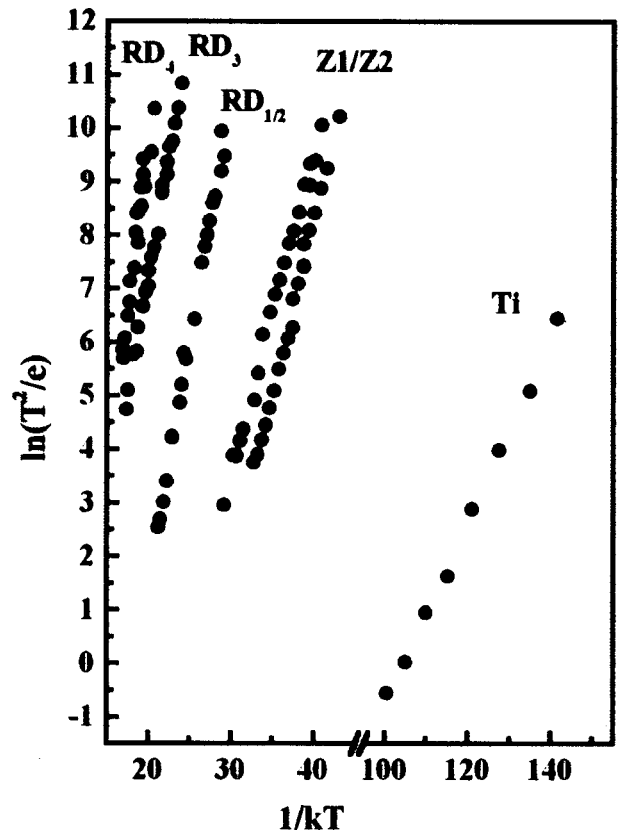

FIG. 3. Arrhenius plot for the traps in 4H–SiC. The trap energies, capture cross sections, and concentrations if present are listed in Table I for the three C/Si ratios.

Z1/Z2 *a* and Z1/Z2 *b*. The square of the capacitance is plotted and fit versus time according to

$$C(t,T)^2 = \frac{q\varepsilon(n_s - \sum N_T)}{2(\varphi_{bi} + V - kT/q)} = A_0 + \sum_i A_i \exp(- t/\tau_i),$$

where n_s is the shallow carrier concentration, N_T is the trap concentration, φ_{bi} is the built in potential, k is Boltzmann's constant, ε is the permittivity, and q is the electron charge. The second part of the equation is the form that is used for fitting, where i is the number of exponential components, and A_0 is the offset. The Levenberg–Marquardt nonlinear least-squares error method was used to fit the transients.[8] An example of the quality of fit, comparing fits for one and two exponential components to the data for the sample with C/Si of three, is given in Fig. 4. The mean square error for a fit assuming one exponential component is 34 times larger than the mean square error for a fit assuming two exponential components at 318 K.

The peak at 320 K is expected to be a double acceptor, and other studies have also identified the peak as an overlapping acceptor trap, but extracting the trap characteristics has been difficult.[9,10] The concentration of the lower-energy trap, which appears at a higher temperature due to the differences in capture cross section, does not change appreciably with C/Si. The higher energy trap, Z1/Z2 *b*, decreases as the C/Si increases from one to three, and is below the sensitivity limit of $5 \times 10^{11}/\text{cm}^3$ for the C/Si of six. In Ref. 9, the peak was partially annealed, reduced to a minimum of 80% at 750 °C. From theoretical work, the peak at 320 K is possibly due to a dicarbon interstitial complex next to a nitrogen interstitial.

TABLE I. Trap energies, capture cross sections, and concentrations measured by DLTS for 4H–SiC grown with C/Si of one, three, and six.

	Ti	Z1/Z2a	Z1/Z2b	RD$_{1/2}$	RD$_3$	RD$_4$
E_T (eV)	0.171	0.582	0.654	0.92	0.89	1.24
σ (cm^2)	7×10^{-14}	3×10^{-15}	1×10^{-13}	4×10^{-14}	8×10^{-17}	7×10^{-15}
C/Si			N_T (cm^{-3})			
1	5×10^{12}	5×10^{12}	1.5×10^{13}			
3	2×10^{12}	5×10^{12}	1.0×10^{13}			
6	5×10^{12}	5×10^{12}		1×10^{12}	9×10^{11}	1×10^{12}

However, other experimental work where the authors used a Si-face SiC instead of a C-face SiC as used here, in addition to the results given here, shows that increasing the carbon decreases the height of this peak, suggesting that the defect may be due to Si$_C$ or V$_C$.[11] Experimental results that diverge from theoretical predictions may indicate that the epitaxy takes place under strongly nonequilibrium conditions. Further clues on the origin are obtained from the field dependence of the trap to confirm the expected acceptor nature. If the trap is charged when empty, the Coulomb potential profile is shifted by the electric field.[12] There was very little field dependence, less than 10% of what it should be for a singly charged defect. From this result, we can conclude that the defect is an acceptor, as determined also by others.[13] Increasing the C/Si ratio also caused other traps at a higher energy to emerge. RD$_{1/2}$, RD$_3$, and RD$_4$ were only seen in appreciable concentrations in the sample grown with C/Si of six. There was some evidence of a higher-energy trap in the samples grown with a C/Si of one and three at temperatures above 700 K for the ratewindow of 228/s. However, the trap parameters could not be determined.

This series of samples, including carbon to silicon ratios of one, three, and six, demonstrated that one of the primary defects in 4H–SiC is related to a carbon vacancy, as determined by a reduction in the Z1/Z2 DLTS peak height with higher C/Si ratio. This result opposes predictions of carbon interstitial components, and supports assignment to a silicon antisite or carbon vacancy relationship. The Z1/Z2 peak was also deconvolved into two component traps, one of which was independent of the C/Si ratio, perhaps related to an impurity in an interstitial site. The *I-V* data showed that the intermediate C/Si ratio of three had lower reverse bias leakage current. The slight increase in leakage current for the C/Si of six reflects the presence of deeper traps seen by DLTS in this sample, which can reduce the thermal barrier through the Schottky barrier by tunneling into the deep levels.
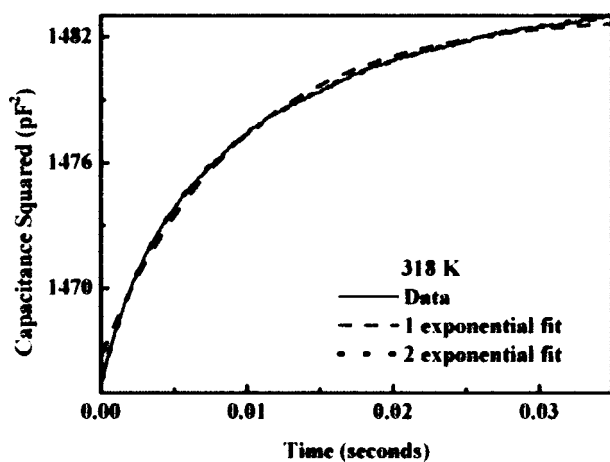
FIG. 4. Representative fit for transient for sample with C/Si of three showing the best fit for two exponential components for the peak appearing at 320 K in the ratewindow plot of Fig. 2. The fit for two components overlaps with the experimental data.

[1] T. A. G. Eberlein, R. Jones, and P. R. Briddon, Phys. Rev. Lett. **90**, 225502 (2003).
[2] A. Kawasuso, F. Redmann, R. Krause-Rehberg, M. Weidner, T. Frank, G. Pensl, P. Sperr, W. Triftshauser, and H. Itoh, Appl. Phys. Lett. **79**, 3950 (2001).
[3] A. Broniatowski, A. Blosse, P. C. Srivastava, and J. C. Bourgoin, J. Appl. Phys. **54**, 2907 (1983).
[4] D. Lang, J. Appl. Phys. **45**, 3023 (1974).
[5] L. Stolt and K. Bohlin, Solid-State Electron. **28**, 1215 (1985).
[6] T. Dalibor, G. Pensl, H. Matsunami, T. Kimoto, W. J. Choyke, A. Shoner, and N. Nordell, Phys. Status Solidi A **162**, 199 (1997).
[7] M. Weidner, T. Frank, G. Pensl, A. Kawasuso, H. Itoh, and R. Krause-Rehberg, Physica B **308**, 633 (2001).
[8] *Numerical Recipes in C, The Art of Scientific Computing* (Cambridge University Press, New York, 1988).
[9] C. Hemmingsson, N. T. Son, O. Kordina, J. P. Bergman, E. Janzen, J. L. Lindstrom, S. Savage, and N. Nordell, J. Appl. Phys. **81**, 6157 (1997).
[10] C. G. Hemmingsson, N. T. Son, A. Ellison, J. Zhang, and E. Janzen, Phys. Rev. B **58**, R10119 (1998).
[11] K. Fujihira, T. Kimoto, and H. Matsunami, J. Cryst. Growth **255**, 136 (2003).
[12] W. R. Buchwald and N. M. Johnson, J. Appl. Phys. **64**, 958 (1988).
[13] T. Dalibor, C. Peppermuller, G. Pensl, S. Sridhara, R. P. Devaty, W. J. Choyke, A. Itoh, T. Kimoto, and H. Matsunami, Inst. Phys. Conf. Ser. **142**, 517 (1996).